Dimensional crossover in the upper critical field of layered superconductors

T. Schneider* and A. Schmidt
IBM Research Division, Zurich Research Laboratory, 8803 Rüschlikon, Switzerland
(Received 9 July 1992)

Using the recently introduced g_3 model for layered superconductors, we calculate the angular and temperature dependence of the upper critical field H_{c2}. By lowering the temperature we find a crossover from three-dimensional bulk behavior to decoupled two-dimensional layers in both the temperature and angular dependence of H_{c2}. This behavior is remarkably consistent with recent experiments and the comparison with the measured angular dependence provides an estimate for the interlayer coupling g_3.

I. INTRODUCTION

Dimensional crossover from three-dimensional (3D) to lower-dimensional behavior in layered superconductors has been the subject of detailed studies for years.[1-10] Layered superconductors include naturally occurring layered compounds, e.g., intercalated transition-metal dichalcogenides, cuprate superconductors, and artificial superlattices. An unavoidable consequence of layered superconductors is the pronounced anisotropy, examples of which include the penetration depth, the Ginzburg-Landau (GL) correlation length, the upper critical field, and the conductivity. Indeed, measuring a given property parallel and perpendicular to the layers yields a ratio markedly different from 1. In particular, the amplitude of the GL correlation length perpendicular to the sheets turns out to be much smaller than the parallel one. In view of this, a dimensional crossover from 3D to 2D behavior should occur at an intermediate temperature above or below the transition temperature T_c. This intermediate temperature can be estimated by equating the GL correlation length perpendicular to the layers, $\xi_\perp(T)=\xi_\perp^0(1-T/T_c)^{-1/2}$, to an appropriate spacing. In YBCO, $\xi_\perp^0\approx 3.36$ Å is less than the distance between the closest CuO_2 planes and considerably smaller than the lattice constant $D\approx 12$ Å perpendicular to the sheets. Thus, by lowering the temperature, crossover behavior is expected to occur around the reduced temperature $t^*=1-T^*/T_c\approx 0.08$, where $\xi_\perp(t^*)=\xi_\perp^0(t^*)^{-1/2}=12$ Å. Related phenomena occur in a film whose thickness becomes comparable to $\xi_\perp$ at some temperature below the bulk transition temperature. Such a system will show its finite extent in one direction and a crossover to nearly 2D behavior.[11-13] Recently, it became possible to fabricate and characterize artificial multilayers containing ultrathin slabs of YBCO, M unit cells thick and separated by N unit cells PrBCO, which are supposed to be insulating.[8-10] It has been shown that a YBCO sheet with nominal thickness of one unit cell is superconducting. However the transition temperature of thin and decoupled YBCO slabs decreased with reduced thickness, accompanied by a broadened resistive transition and a much lower zero resistance temperature.[8-10] Moreover, the fall of the transition temperature for M YBCO unit cells separated by N PrBCO units with N clearly reveals the importance of an interlayer interaction leading to 3D bulk behavior. In this context it is important to recognize that the standard GL theory, which adopts an anisotropic continuum description, is valid only as long as the shortest correlation length is large compared to the appropriate lattice spacing. Indeed, it is assumed that the order parameter varies slowly on the scale of the lattice spacing. In layered systems, however, where $D>\xi_\perp^0$, the dimensional crossover occurs outside of the range of validity of the standard theory. Variations of the order parameter on the scale of the lattice spacing perpendicular to the layers can be taken into account by adopting a discrete description along this direction. However, within the framework of the GL theory, the discretization is not unique and also depends on the properties of the intervening sheets which might be of normal metallic or insulating nature. In what follows we assume insulating intervening layers. Moreover, the superconducting slabs might be treated as infinitely thin or as having a thickness d. For infinitely thin superconducting sheets, there is the model proposed by Lawrence and Doniach (LD model),[14] which has the free-energy density

$$f_l=\frac{\hbar^2}{2M_\parallel}\left|\left(\nabla_\parallel-i\frac{2\pi}{\Phi_0}\mathbf{A}_\parallel\right)\psi_l(\mathbf{r}_\parallel)\right|^2+\alpha|\psi_l(\mathbf{r}_\parallel)|^2+\frac{\beta}{2}|\psi_l(\mathbf{r}_\parallel)|^4+\frac{\hbar^2}{2M_\perp s^2}|\psi_{l+1}(\mathbf{r}_\parallel)e^{-i(2\pi/\Phi_0)\overline{A}_\perp s}-\psi_l(\mathbf{r}_\parallel)|^2 \quad (1)$$

and the free energy

$$F=s\sum_l\int d\mathbf{r}_\parallel f_l\ , \quad (2)$$

where l labels the superconducting layers separated by insulating sheets of thickness s. In the z direction, which is perpendicular to the layers, the order parameter ψ_l is discrete and within the superconducting sheets it depends continuously on $\mathbf{r}_\parallel=(x,y)$. $\mathbf{A}=(\mathbf{A}_\parallel,A_\perp)$ is the vector potential and $\overline{A}_\perp$ is

$$\overline{A}_\perp=\frac{1}{s}\int_{ls}^{(l+1)s}dz\,A_\perp\ . \quad (3)$$

The fourth term is a discrete version of the gradient term along z, the direction perpendicular to the layers. Microscopically it arises from electron single-particle tunneling through the insulating sheets. Accordingly, the effective mass $M_\perp$ is related to the tunneling matrix element by

$$\frac{\hbar^2}{2M_\perp s} \sim t^2 . \tag{4}$$

Thus, this interlayer interaction has a definite sign, and considering only phase fluctuations, is equivalent to Josephson coupling.[14] Moreover, the coupling has to be small, otherwise the single-particle interlayer tunneling must be incorporated in the band structure.

Based on a microscopic analysis of the interlayer interactions, Schneider, Gedik, and Ciraci proposed a model (g_3 model),[11] which differs on the GL level in the discretization of the gradient term in the direction perpendicular to the layers. In this model the free-energy density is given by

$$f_l = \frac{\hbar^2}{2M_\parallel}\left|\left[\nabla_\parallel - i\frac{2\pi}{\Phi_0}\mathbf{A}_\parallel\right]\psi_l(\mathbf{r}_\parallel)\right|^2 + \alpha|\psi_l(\mathbf{r}_\parallel)|^2 + \frac{\beta}{2}|\psi_l(\mathbf{r}_\parallel)|^4 - \frac{g_3}{2}\{\psi_l^*(\mathbf{r}_\parallel)[\psi_{l+1}(\mathbf{r}_\parallel)e^{-i(2\pi/\Phi_0)\bar{A}_\perp s} + \psi_{l-1}(\mathbf{r}_\parallel)e^{i(2\pi/\Phi_0)\bar{A}_\perp s}] + \text{c.c.}\} . \tag{5}$$

Microscopically, g_3 describes an electron interlayer interaction. As a consequence, it can adopt either sign and is not restricted to weak coupling. In the continuum limit, this model leads to the standard GL form as well, with

$$\frac{\hbar^2}{2M_\perp s^2} = |g_3| , \quad \alpha \to \alpha - 2|g_3| , \tag{6}$$

where α and in turn T_c becomes renormalized. The resulting enhancement of T_c does not depend on the sign of g_3, which only affects the phase of the order parameter in the direction perpendicular to the superconducting slabs. In fact, the repulsive ($g_3 < 0$) and attractive case differ only in the phase of the order parameter. For $g_3 < 0$ the order parameter is staggered and the phase differs from layer to layer by π. These features open an interesting scenario, including superconductivity mediated or enhanced by a repulsive interlayer electron interaction with an order parameter differing from layer to layer in its phase. A weakness of both models is the assumption of infinitely thin superconducting slabs. Indeed, this limit leads to artificial results for the parallel upper critical field.[15] This unrealistic limit is readily removed by considering slabs of finite thickness d. In this case the free energy of the g_3 model [Eqs. (2) and (5)] reads

$$F = \sum_l \int d\mathbf{r}_\parallel \left\{ \int_{lD-d/2}^{lD+d/2} dz \left[\frac{\hbar^2}{2M_\parallel}\left|\left[\nabla_\parallel - i\frac{2\pi}{\Phi_0}\mathbf{A}_\parallel\right]\psi_l(\mathbf{r}_\parallel,z)\right|^2 + \frac{\hbar^2}{2M_\perp}\left|\left[\nabla_\perp - i\frac{2\pi}{\Phi_0}A_\perp\right]\psi_l(\mathbf{r}_\parallel,z)\right|^2 + \alpha|\psi_l(\mathbf{r}_\parallel,z)|^2 + \frac{\beta}{2}|\psi_l(\mathbf{r}_\parallel,z)|^4 \right] - \frac{dg_3}{2}\{\psi_l^*(\mathbf{r}_\parallel, lD+d/2)\psi_{l+1}[\mathbf{r}_\parallel,(l+1)D-d/2]e^{-i(2\pi/\Phi_0)\bar{A}_\perp s} + \psi_l^*(\mathbf{r}_\parallel, lD-d/2)\psi_{l-1}[\mathbf{r}_\parallel,(l-1)D+d/2]e^{i(2\pi/\Phi_0)\bar{A}_\perp s} + \text{c.c.}\} \right\} . \tag{7}$$

The constant d denotes the thickness of the superconducting slabs separated by insulating material of thickness s (compare Fig. 1). Thus $D = d + s$ is the lattice constant in the z direction and

$$\bar{A}_\perp = \frac{1}{s}\int_{lD+d/2}^{(l+1)D-d/2} dz\, A_\perp . \tag{8}$$

A corresponding version of the LD model has been proposed by Deutscher and Entin-Wohlman.[15]

In this paper we explore the temperature and angular dependence of the upper critical orbital field for the g_3 model as defined in Eq. (7).

II. CALCULATION OF THE UPPER CRITICAL FIELD

To calculate the upper critical field and its angular dependence we adopt the gauge

$$\mathbf{A} = H(0, x\cos\vartheta, x\sin\vartheta) \tag{9}$$

corresponding to

$$\mathbf{H} = H(0, \sin\vartheta, \cos\vartheta) . \tag{10}$$

We assume that d is small compared to the screening length λ and $d < \xi_\perp$. The first limit assures that we can neglect screening currents and hence we can treat the magnetic field as uniform. For $d < \xi_\perp$ the magnitude of

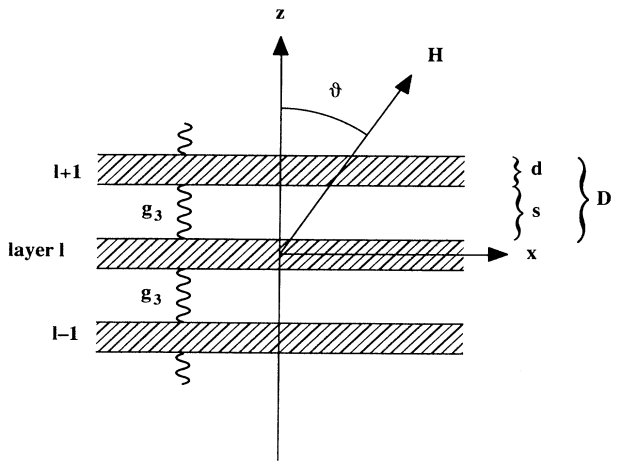

FIG. 1. Schematic picture of the layered model system. Superconducting slabs of thickness d, coupled by the g_3 term, are separated by insulating material.

the order parameter is nearly constant within a superconducting slab. Following Deutscher and Entin-Wohlman[15] we thus choose a solution of the form

$$\psi_l(x,y,z)=u(x,y)e^{iF_l(x,z)} . \tag{11}$$

Substitution into Eq. (7) leads to the gradient term

$$\left[\frac{\partial}{\partial z}-i\frac{2\pi}{\Phi_0}A_z\right]\psi_l=iu\left[\frac{\partial F_l}{\partial z}+\frac{2\pi}{\Phi_0}Hx\sin(\vartheta)\right]e^{iF_l} . \tag{12}$$

To avoid arbitrary growth in this term for large x, we choose the phase in the form

$$F_l=-\frac{2\pi}{\Phi_0}Hx\sin(\vartheta)(z-z_l) , \tag{13}$$

where z_l is chosen to minimize the free energy, yielding $z_l=lD$. By this Eq. (7) reduces to

$$F=d\sum_l\int d\mathbf{r}_\parallel\left\{\frac{\hbar^2}{2M_\parallel}\left[\left|\frac{\partial}{\partial x}u\right|^2+\frac{d^2}{12}\left|\frac{2\pi}{\Phi_0}H\sin(\vartheta)u\right|^2+\left|\left[\frac{\partial}{\partial y}-i\frac{2\pi}{\Phi_0}Hx\cos(\vartheta)\right]u\right|^2\right]\right.$$
$$\left.+\alpha|u|^2+\frac{\beta}{2}|u|^4-2|g_3|\cos\left[\frac{2\pi}{\Phi_0}Hx\sin(\vartheta)D\right]|u|^2\right\} , \tag{14}$$

where we take the absolute value of g_3 because of the possibility of a staggered order parameter as explained above. Assuming that u is independent of y, variation of Eq. (14) with respect to u leads to

$$-\frac{\hbar^2}{2M_\parallel}\left[\frac{d^2}{dx^2}+\frac{d^2}{12}\left[\frac{2\pi}{\Phi_0}H\sin(\vartheta)\right]^2+\left[\frac{2\pi}{\Phi_0}Hx\cos(\vartheta)\right]^2\right]u+\left[\alpha-2|g_3|\cos\left[\frac{2\pi}{\Phi_0}Hx\sin(\vartheta)D\right]\right]u=0 , \tag{15}$$

where we have neglected the quartic term. This ordinary differential equation corresponds to a generalized Mathieu equation

$$\left[\frac{d^2}{d\bar{x}^2}+a+2q\cos(2\bar{x})-p\bar{x}^2\right]u=0 \tag{16}$$

with

$$\bar{x}=\frac{\pi}{\Phi_0}HD\sin(\vartheta)x ,$$
$$p=\left[\frac{2\Phi_0}{\pi H}\frac{\cos(\vartheta)}{D^2\sin^2(\vartheta)}\right]^2 ,$$
$$q=\frac{2M_\parallel}{\hbar^2}\left[\frac{\Phi_0}{\pi HD\sin(\vartheta)}\right]^2|g_3| , \tag{17}$$
$$a=-\frac{d^2}{3D^2}-\frac{2M_\parallel}{\hbar^2}\left[\frac{\Phi_0}{\pi HD\sin(\vartheta)}\right]^2\alpha ,$$

which reduces for magnetic field parallel to the layers ($\vartheta\to\pi/2, p\to 0$) to the normal Mathieu equation. Finding the upper critical field H_{c2} corresponds then to evaluating the lowest eigenvalue $a_0(p,q)$ of Eq. (16).

III. RESULTS AND COMPARISON WITH EXPERIMENTS

We first examine the upper critical field $H_{c2}^\parallel$ parallel to the layers as a function of temperature and then turn to the angular dependence of H_{c2}.

If the magnetic field is parallel to the layers, Eq. (16) reduces to the Mathieu equation. In the high- ($q\to 0$) and low- ($q\to\infty$) field limit, the lowest eigenvalue a_0 is given by

$$a_0=-\tfrac{1}{2}q^2\to 0 \tag{18}$$

or

$$a_0=-2q+2\sqrt{q} . \tag{19}$$

From this and Eq. (17) we obtain for high fields

$$H_{c2}^\parallel=\frac{\Phi_0}{2\pi}\frac{\sqrt{12}}{\xi_\parallel^s d} \tag{20}$$

with

$$\frac{1}{(\xi_\parallel^s)^2}=-\frac{2M_\parallel}{\hbar^2}\alpha . \tag{21}$$

From the latter definition we see that $\xi_{\parallel}^{s}$ is the correlation length for a single slab.

For low fields we get

$$H_{c2}^{\parallel}=\frac{\Phi_0}{2\pi}\frac{1}{\xi_{\parallel}\xi_{\perp}} \tag{22}$$

with

$$\frac{1}{\xi_{\parallel}^2}=\frac{2M_{\parallel}}{\hbar^2}(-\alpha+2|g_3|)=\frac{1}{(\xi_{\parallel}^0)^2}\left[1-\frac{T}{T_c}\right],$$
$$\frac{\xi_{\perp}}{\xi_{\parallel}}=\left[\frac{M_{\parallel}}{M_{\perp}}\right]^{1/2}. \tag{23}$$

Thus, as the magnetic field is increased, the temperature dependence crosses over from linear to square-root behavior because $\xi\propto(1-T/T_c)^{-1/2}$.

To obtain the full temperature dependence we solved the Mathieu equation numerically. The result for $a_0(q)$ is shown in Fig. 2 together with the limiting behavior for high and low fields [Eqs. (18) and (19)].

To extract the temperature dependence of H_{c2}, the parameters d, D, $\xi_{\parallel}^0$, and $M_{\perp}/M_{\parallel}$ must be fixed. Figure 3(a) shows $H_{c2}^{\parallel}(T)$ for parameters representative of YBCO, namely[16]

$$d=3.35\ \text{Å}\ ,\quad D=12\ \text{Å}\ ,$$
$$M_{\perp}/M_{\parallel}=(7.9)^2\ ,\quad \xi_{\parallel}^0=20\ \text{Å}\ . \tag{24}$$

The crossover in the temperature dependence from linear to square-root behavior is clearly seen and occurs around $t=1-T/T_c=0.1$. This is close to the temperature T^*, where $\xi_{\perp}$ reaches the lattice constant D,

$$\xi_{\perp}=\left[\frac{M_{\parallel}}{M_{\perp}}\right]^{1/2}\xi_{\parallel}^0\left[1-\frac{T^*}{T_c}\right]^{-1/2}=D\ . \tag{25}$$

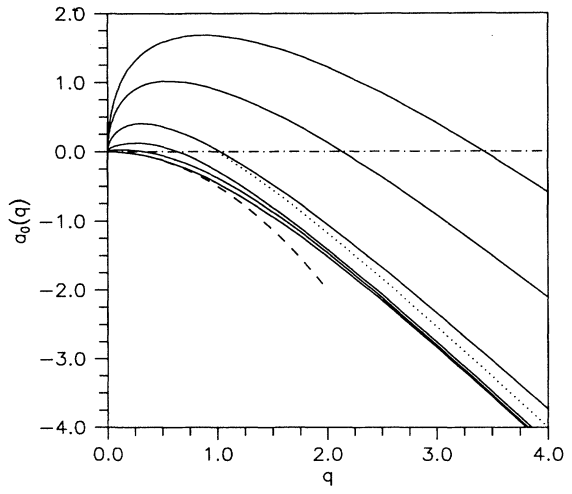

FIG. 2. The solid lines are solutions $a_0(p,q)$ of the generalized Mathieu equation (16) with fixed $r=p/q$ (corresponding to fixed angle ϑ). From bottom to top: $r=0$, 0.01, 0.1, 1, 5, and 10. The limiting behavior for the Mathieu equation ($p=r=0$) given in Eqs. (18) and (19) is shown as a dashed (dotted) line.

Thus, below T^* the system corresponds to nearly decoupled slabs.

In BiSCO (2212) the fit of the anisotropy and $\xi_{\parallel}^0$ to the experimental angular dependence (see below) leads to

$$d=3.35\ \text{Å}\ ,\quad D=18.35\ \text{Å}\ ,$$
$$M_{\perp}/M_{\parallel}=(54.5)^2\ ,\quad \xi_{\parallel}^0=145\ \text{Å} \tag{26}$$

with $M_{\perp}/M_{\parallel}$ very close to the value given in Ref. 17. The resulting temperature dependence of H_{c2} is shown in Fig. 3(b). Due to the large anisotropy, the region where the linear temperature dependence occurs, corresponding to 3D behavior, is seen to be quite small. Indeed, Eq. (25) yields in this case

$$t^*=1-T^*/T_c=0.021\ . \tag{27}$$

Next we turn to the angular dependence of H_{c2}. In the

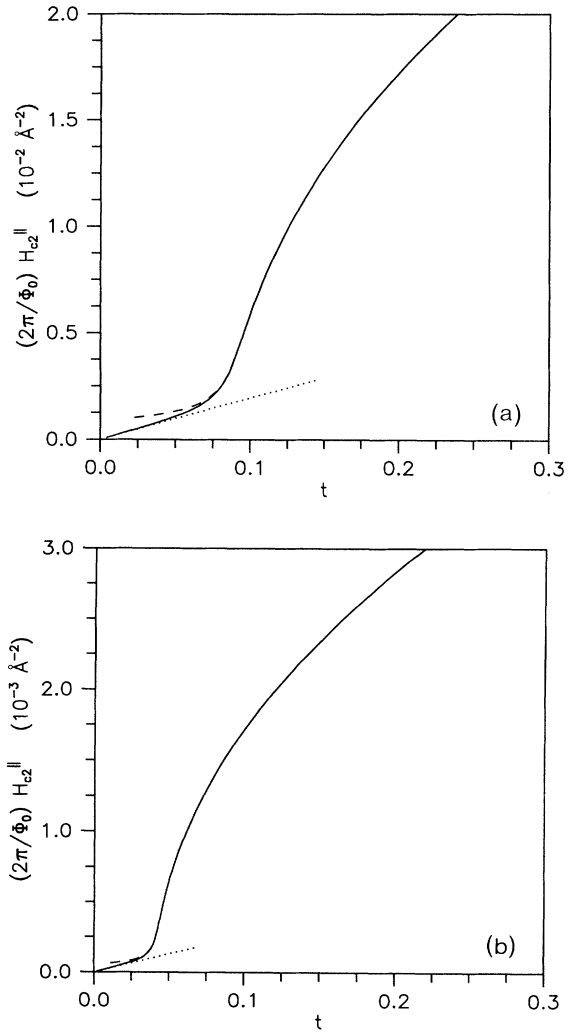

FIG. 3. Upper critical field $H_{c2}^{\parallel}$ vs reduced temperature $t=1-T/T_c$ for (a) YBCO: $d=3.35$ Å, $D=12$ Å, $M_{\perp}/M_{\parallel}=(7.9)^2$, and $\xi_{\parallel}^0=20$ Å; (b) BiSCO: $d=3.35$ Å, $D=18.35$ Å, $M_{\perp}/M_{\parallel}=(54.5)^2$, and $\xi_{\parallel}^0=145$ Å.

low- and high-field limits, Eq. (15) can be solved exactly. Indeed, for low fields the cosine term can be expanded and one regains the standard effective-mass expression for the angular dependence,[18]

$$\frac{H_{c2}(\vartheta)\sin^2(\vartheta)}{(H_{c2}^{\parallel})^2}+\frac{H_{c2}(\vartheta)\cos^2(\vartheta)}{(H_{c2}^{\perp})^2}=1\ , \tag{28}$$

with $H_{c2}^{\parallel}$ of (22) and

$$\frac{H_{c2}^{\perp}}{H_{c2}^{\parallel}}=\left[\frac{M_{\parallel}}{M_{\perp}}\right]^{1/2}\ . \tag{29}$$

For sufficiently high fields, however, the cosine term can be neglected. The resulting angular dependence is

$$\frac{H_{c2}^2(\vartheta)\sin^2\vartheta}{(H_{c2}^{\parallel})^2}+\frac{H_{c2}(\vartheta)|\cos\vartheta|}{H_{c2}^{\perp}}=1\ , \tag{30}$$

where

$$H_{c2}^{\parallel}=\frac{\Phi_0}{2\pi}\frac{\sqrt{12}}{\xi_{\parallel}^{s}d}\ ,\quad H_{c2}^{\perp}=\frac{\Phi_0}{2\pi}\frac{1}{(\xi_{\parallel}^{s})^2}\ . \tag{31}$$

The absence of the interlayer coupling g_3 reveals that sufficiently strong fields decouple the superconducting slabs. Indeed expression (31) is equivalent to that for an isolated thin slab of thickness d.[18] From Eqs. (28) and (30) it is seen that the crossover from 3D bulk to 2D slab behavior is most pronounced around $\vartheta=\pi/2$, corresponding to a magnetic field applied parallel to the layers. In the 3D case, Eq. (28) yields

$$\left.\frac{dH_{c2}}{d\vartheta}\right|_{\vartheta=\pi/2}=0 \tag{32}$$

while the 2D slab behavior Eq. (30) gives

$$\left.\frac{dH_{c2}}{d\vartheta}\right|_{\vartheta=\pi/2}=\pm\frac{(H_{c2}^{\parallel})^2}{2H_{c2}^{\perp}}\neq 0 \tag{33}$$

so that $H_{c2}(\vartheta)$ will have a cusp at $\vartheta=\pi/2$.

For intermediate field strength one has to solve Eq. (15) or the generalized Mathieu equation (16). The numerical solution turns out to be nontrivial, because for $\vartheta\neq\pi/2$ one has the term $-p\bar{x}^2$ and the solutions change from periodic to bounded. Solutions $a_0(p,q)$ of the generalized Mathieu equation (16) are plotted in Fig. 2 for various ratios of p and q corresponding via (17) to different fixed angles ϑ. From these data the angular dependence of the upper critical field can now be extracted. In Fig. 4 we depicted $H_{c2}(\vartheta)/H_{c2}^{\parallel}$ versus ϑ for several reduced temperatures t. For comparison we included the limiting behavior for small and large reduced temperature. Apparently there is excellent agreement in the appropriate limits. In the crossover region from the limiting 3D to the 2D behavior the curves first develop a very sharp cusp on the top of a broader peak ($t=0.03, 0.04, 0.05$), followed by a sharpening up to $t\approx 0.1$. As t increases further, the peak broadens and approaches the 2D cusp shape.

Measurements of the upper critical field are complicated by the following facts: The usual resistivity and ac methods seem to measure a field H^* determined by the dissipation due to the onset of flux motion. In natural high-temperature superconductors, for which the crystal structure is fixed, the crossover can be observed only by changing the temperature. Due to the extremely high value of the derivative dH_{c2}/dT just below T_c, an unambiguous investigation of the crossover is difficult. Thus, in order to unravel the anisotropy and discreteness effects in the bulk, alternative methods have been used. Experimental evidence for a magnetic-field-induced dimensional crossover in bulk YBCO was found by Farrell *et al.* by means of torque measurements,[16] and in BiSCO (2212) in terms of the angular dependence of H^*.[5,6] Moreover, the anisotropy ratio $H_{c2}^{\parallel}/H_{c2}^{\perp}$ as determined from torque and magnetization measurements agree reasonably well with the estimates obtained from the field $H^*(\vartheta)$ for the onset of dc resistivity. Some estimates are listed in Table I.

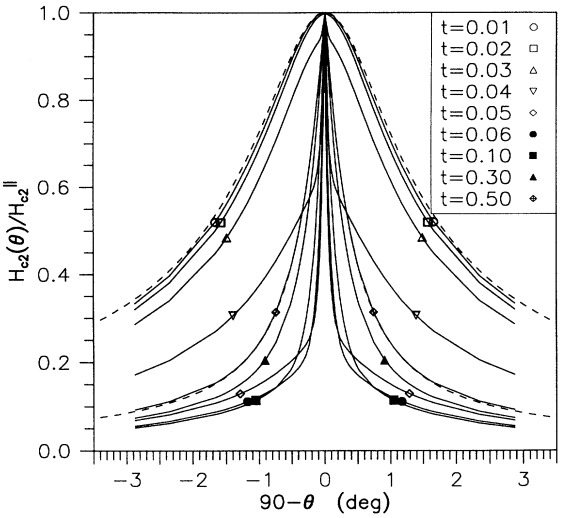

FIG. 4. Angular dependence of the upper critical field H_{c2}: Solutions of Eq. (15) with the parameters of BiSCO [as in Fig. 3(b)] for different reduced temperatures t. The angle ϑ is given in degrees. The dashed lines show the limiting 3D and 2D behavior of Eqs. (28) and (30), respectively.

In view of this, the anisotropy of H^* appears to be close to that of the intrinsic H_{c2}. The angular dependence of H^* has been studied in bulk YBCO at 89 and 84.5 K with $T_c=91.2$ K, yielding $H_{\parallel}^*/H_{\perp}^*=8.5$.[20] Within the rather limited angular resolution, the data agree well with the effective-mass formula (28). These findings are consistent with our estimate in Eq. (25), which yields $T_c=91.2$ K, $T^*=79.3$ K. In contrast to these results, the data for BiSCO with $T_c=82$ K were found to agree much better with the thin-film formula (30) at $T=80.4$ K.[20] These results are consistent with

TABLE I. Estimates for $H_{c2}^{\parallel}/H_{c2}^{\perp}$ from the onset of resistivity, magnetic torque, and magnetization measurements.

Experiment	YBCO	BiSCO (2212)
Resistivity	8.5 (Ref. 20)	56 (Ref. 20)
Torque	7.9 (Ref. 16)	55 (Ref. 17)
Magnetization	6 (Ref. 19)	

our estimate for T^* in (27) and imply nearly 2D behavior rather close to T_c. Recently, the angular and temperature dependence of H^* in BiSCO has been studied with much better angular resolution. In one sample with $T_c=79.1$ K (sample I of Ref. 6), measurements of $H^*(\vartheta)$ have been performed at 78 and 76 K. The results are depicted in Fig. 5. With $M_\parallel/M_\perp=(54.5)^2$ and $\xi_\parallel^0=145$ Å the appropriate solution of (15) correctly reflects the experimental ratios $H_{c2}^\perp/H_{c2}^\parallel$ (Fig. 6) and the angular dependence of the solutions is quite close to the data. We find that for $T=78$ K ($t=0.014$) the solution is not very different from the 3D bell shape, whereas for $T=76$ K ($t=0.04$) the 2D formula (30) is not yet applicable for our parameters, because $1/(\xi_\parallel^s)^2=-2M_\parallel/\hbar^2\alpha$ is still negative. Thus this temperature is too high and real 2D behavior cannot be observed, although the solution of (15) exhibits a sharp cusp around $\vartheta=0$. For intermediate temperature ($76<T<78$ K) the measured $H^*(\vartheta)$ exhibits a sharp cusp on top of a broad peak.[7] This finding is very similar to the behavior shown in Fig. 4 for $t=0.3,0.4$. The limited experimental resolution in ϑ, however, does not allow a more quantitative comparison.

As discussed above [Eqs. (22) and (20)] and illustrated in Fig. 3, it is clear that the crossover in the angular dependence of H^* is accompanied by a crossover in $H^*(T)$ from linear to square-root behavior. The data for $H^*(T)$ of Ref. 6 confirm this behavior qualitatively, but more extended and precise measurements are needed for a detailed comparison.

Nevertheless, the parameters derived from the data of sample I, namely $T^*=77.8$ K, $T_c=79.1$ K, can be used to estimate the amplitude of the GL correlation length with Eq. (25). Together with $H_\parallel^*/H_\perp^*=\sqrt{M_\perp/M_\parallel}=\xi_\parallel/\xi_\perp=54.5$, this yields

$$\xi_\parallel^0=128\ \text{Å}\ ,\quad \xi_\perp^0=2.35\ \text{Å}\ . \tag{34}$$

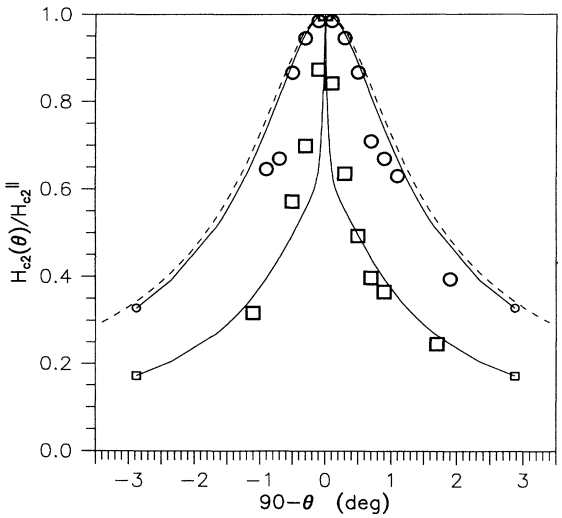

FIG. 5. Comparison of the solution to Eq. (15) with experimental data (H^* of Ref. 6) for a sample of BiSCO with $T_c=79.1$ K [parameter as in Fig. 3(b)]. ○ at $T=78$ K, □ at $T=76$ K. The dashed line shows the 3D behavior (30).

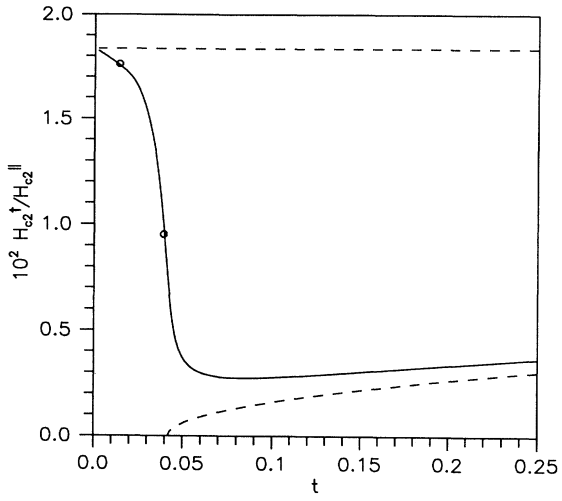

FIG. 6. $H_{c2}^\perp/H_{c2}^\parallel$ vs reduced temperature t. The solution of (15) with the parameters of BiSCO (26) is shown as a solid line and fits to the two experimental points of Ref. 6. Dashed lines show the limiting 3D and 2D behavior resulting from (29) and (31), respectively.

The value of $\xi_\parallel^0$ is much larger than previous estimates, but is close to our fitted value (26). In this context it should be emphasized that $\xi_\parallel^0$ is the amplitude of the correlation length divergence *close to the bulk transition.* $\xi_\perp^0=2.35$ Å is, however, of the expected order of magnitude. Thus the value of $\xi_\parallel^0$ simply reflects the large effective-mass anisotropy.

IV. SUMMARY

On the basis of the g_3 model [Eq. (14)] we derived an ordinary differential equation from which the upper critical field $H_{c2}(T,\vartheta)$ can be calculated. Close to T_c and at low temperature an exact solution is possible and one regains the standard effective-mass expression and the thin slab formula, respectively.[18] In the intermediate temperature regime we solved the equation numerically to explore the crossover between these limiting behaviors in both the temperature (from linear to square root) and angular dependence (from bell-shaped to cusplike) of H_{c2}. This corresponds to the crossover from a bulk superconductor to decoupled thin slabs as the temperature is lowered. The temperature T^* of the decoupling is approximately reached when the perpendicular GL coherence length $\xi_\perp(T)$ is close to the distance of the superconducting slabs D. The remaining parameters ($M_\perp/M_\parallel$ and $\xi_\parallel^0$) have been estimated from the measured temperature and angular dependence of H^*. Good agreement is obtained for $M_\perp/M_\parallel=(54.5)^2$, consistent with magnetic torque measurements (Table I) and $\xi_\parallel^0=145$ Å. This rather large value is consistent, however, with $\xi_\perp^0\approx 2-3$ Å ($\xi_\perp^0=\sqrt{M_\parallel/M_\perp}\xi_\parallel^0$). Using these estimates and $M_\parallel=3m_e$, we obtain $g_3=0.05$ meV for the interlayer coupling constant, in agreement with the value we deduced from the

crossover analysis of measured specific heat and conductivity.[21] Finally we note that the agreement between our mean-field results and experiments is quite remarkable in view of our having neglected fluctuations.

ACKNOWLEDGMENTS

We thank R. Marcon for providing us with his experimental data and D. Ariosa for stimulating discussions.

*Author to whom correspondence may be sent: Bitnet address: TS@ZURLVM1

[1]B. Y. Jin and J. B. Ketterson, Adv. Phys. **38**, 189 (1989).

[2]C. S. L. Chun, G. Zheng, J. L. Vicent, and I. K. Schuller, Phys. Rev. B **29**, 4915 (1984).

[3]I. Banerjee, Q. S. Yang, C. M. Falco, and I. K. Schuller, Phys. Rev. B **28**, 5037 (1983).

[4]D. E. Farrell, J. P. Rice, D. M. Ginsberg, and J. Z. Liu, Phys. Rev. Lett. **64**, 1573 (1990).

[5]R. Fastampa, M. Giura, R. Marcon, and E. Silva, Phys. Rev. Lett. **67**, 1795 (1991).

[6]R. Marcon, R. Fastampa, M. Girua, and E. Silva, Europhys. Lett. **16**, 757 (1991).

[7]R. Marcon, E. Silva, R. Fastampa, and M. Giura, Phys. Rev. B **46**, 3612 (1992).

[8]J. M. Triscone, Ø. Fischer, O. Brunner, L. Antognazza, A. D. Kent, and M. G. Karkut, Phys. Rev. Lett. **64**, 804 (1990).

[9]Q. Li, X. X. Xi, X. D. Wu, A. Inam, S. Vadlamannati, W. L. McLean, T. Venkatesan, R. Ramesh, D. M. Hwang, J. A. Martinez, and L. Nazar, Phys. Rev. Lett. **64**, 3086 (1990).

[10]D. H. Lowndes, D. P. Norton, and J. D. Budai, Phys. Rev. Lett. **65**, 1160 (1990).

[11]T. Schneider, Z. Gedik, and S. Ciraci, Z. Phys. B **83**, 313 (1991).

[12]T. Schneider, Z. Phys. B **85**, 187 (1991).

[13]T. Schneider, Physica C **195**, 82 (1992).

[14]W. E. Lawrence and S. Doniach, in *Proceedings of the 12th International Conference on Low Temperature Physics,* edited by E. Kanda (Academic, Kyoto, Japan, 1971), p. 361.

[15]D. Deutscher and O. Entin-Wohlmann, Phys. Rev. B **17**, 1249 (1978).

[16]D. E. Farrell, C. M. Williams, S. A. Wolf, N. P. Bansal, and V. G. Kogan, Phys. Rev. Lett. **61**, 2805 (1988).

[17]D. E. Farrell, S. Bonham, J. Foster, Y. C. Chang, P. Z. Jiang, K. G. Vandervoort, D. J. Lam, and V. G. Kogan, Phys. Rev. Lett. **63**, 782 (1989).

[18]M. Tinkham, *Introduction to Superconductivity* (Krieger, Malbar, FL, 1980).

[19]U. Welp, W. K. Kwok, G. W. Crabtree, K. G. Vandervoort, and J. Z. Liu, Phys. Rev. Lett. **62**, 1908 (1989).

[20]M. J. Naughton, R. C. Yu, P. K. Davies, J. E. Fischer, R. V. Chamberlin, Z. Z. Wang, T. W. Jing, N. P. Ong, and P. M. Chaikin, Phys. Rev. B **38**, 9280 (1988).

[21]D. Ariosa (private communication).